Identification and structural analysis of type I collagen sites in complex with fibronectin fragments

Michèle C. Erat[a], David A. Slatter[b], Edward D. Lowe[c], Christopher J. Millard[a], Richard W. Farndale[b], Iain D. Campbell[a], and Ioannis Vakonakis[a,1]

[a]Department of Biochemistry and [c]Laboratory of Molecular Biophysics, University of Oxford, Oxford OX1 3QU, United Kingdom; and [b]Department of Biochemistry, University of Cambridge, Cambridge CB2 1QW, United Kingdom

Edited by John Kuriyan, University of California, Berkeley, CA, and approved January 28, 2009 (received for review December 9, 2008)

Collagen and fibronectin are major components of vertebrate extracellular matrices. Their association and distribution control the development and properties of diverse tissues, but thus far no structural information has been available for the complex formed. Here, we report binding of a peptide, derived from the α_1 chain of type I collagen, to the gelatin-binding domain of human fibronectin and present the crystal structure of this peptide in complex with the $^{8-9}$FnI domain pair. Both gelatin-binding domain subfragments, ^{6}FnI$^{1-2}$FnII^{7}FnI and $^{8-9}$FnI, bind the same specific sequence on D-period 4 of collagen I α_1, adjacent to the MMP-1 cleavage site. $^{8-9}$FnI also binds the equivalent sequence of the α_2 chain. The collagen peptide adopts an antiparallel β-strand conformation, similar to structures of proteins from pathogenic bacteria bound to FnI domains. Analysis of the type I collagen sequence suggests multiple putative fibronectin-binding sites compatible with our structural model. We demonstrate, by kinetic unfolding experiments, that the triple-helical collagen state is destabilized by $^{8-9}$FnI. This finding suggests a role for fibronectin in collagen proteolysis and tissue remodeling.

collagen destabilization | extracellular matrix | protein structure

Collagen is the most abundant protein in mammals, accounting for ≈25% of the body-protein content. It is crucial for effects as diverse as cell differentiation, cell migration, and mechanical properties of tissues. Many human diseases have their origin in mutations that affect interactions of collagen with other extracellular matrix (ECM) molecules and cell receptors (1). Type I collagen fibrils form spontaneously in vitro; in vivo, however, formation requires integrin receptors and fibronectin (FN) (2). FN is a large glycosylated protein composed of multiple copies of 3 classes of domains, FnI, FnII, and FnIII, that forms fibrils in the ECM (3). It plays a role in many important physiological processes, such as embryogenesis, wound healing, hemostasis, and thrombosis (4), and disruption of the FN gene is embryonic lethal in mice (5).

The interaction of these 2 proteins has long been demonstrated in vitro by using denatured collagen (gelatin) (6, 7) and isolated collagen type I chains or chain fragments (8, 9). The collagen-binding site on FN has been localized to the 42-kDa gelatin-binding domain (GBD; for an overview of FN and collagen fragments see Fig. 1) (10, 11), and anti-GBD antibodies inhibit collagen organization in fibroblast cultures (12). Similarly, experiments in cultures have identified the collagenase/MMP-1 (13) cleavage site in type I collagen as important for FN-mediated attachment of fibroblasts to collagen ECM (14). Peptides spanning that region (15) or MMP-1 cleavage at this site (6) inhibit attachment. However, attempts to reconstitute the FN–collagen interaction in vitro by using synthetic peptides failed to find strong, specific, interactions (8, 9), and the precise sequence determinants for FN-binding to collagen remained unknown.

Here, we report a tight interaction between GBD and a synthetic peptide from the α_1 chain of collagen type I [α_1(I)], defined by using NMR and fluorescence. Both GBD subfragments bind the same peptide sequence just C-terminal to the MMP-1 cleavage site; the tightest binding, however, is mediated by the $^{8-9}$FnI domain pair that also binds α_2(I). A 2.1-Å crystal structure of $^{8-9}$FnI in complex with the α_1(I) peptide shows an extended single-strand peptide conformation, which suggests that FN stabilizes a noncanonical collagen structure upon binding. We explore this hypothesis in thermal denaturation experiments using model triple-helical peptides. The results presented show the first atomic resolution picture of the interaction between FN fragments and collagen peptides and give insights into a possible role for FN in collagen degradation.

Results and Discussion

GBD Interacts with a Type I Collagen Peptide Adjacent to the MMP-1 Cleavage Site. To explore the FN–collagen interaction, we tested by NMR a series of synthetic single-stranded peptides covering α_1(I) residues G_{763}–R_{816} for binding the 2 subfragments of the GBD, $^{8-9}$FnI and ^{6}FnI$^{1-2}$FnII^{7}FnI. The tested region of collagen spans the MMP-1 cleavage site, G_{775}/I_{776}, which has been shown to influence FN-collagen interactions (6). Of the FN fragments, $^{8-9}$FnI is known to associate with α_1(I) fragments and gelatin (16, 17), and ^{6}FnI$^{1-2}$FnII^{7}FnI binds gelatin more strongly than the shorter ^{6}FnI$^{1-2}$FnII (18). The NMR titrations in this study often resulted in unfavorable intermediate exchange regimes; therefore, we tried to optimize the experimental conditions in each case by using different temperatures and different magnetic field strengths, 500 and 950 MHz. Affinities from these titrations [supporting information (SI) Fig. S1] are summarized in Table S1. Both GBD subfragments only bound tightly to a peptide spanning α_1(I) residues G_{778}–G_{799} (Fig. 2 *A* and *B*), with dissociation constants, K_d, of 5 ± 1 μM for $^{8-9}$FnI (25 °C) and 57 ± 6 μM for ^{6}FnI$^{1-2}$FnII^{7}FnI (37 °C). This peptide, identified as the main binding site for both GBD subfragments, is located just C-terminal to the MMP-1 cleavage site (15). Collagen regions immediately N- or C-terminal to this peptide yielded little or no affinity, and control experiments using $^{4-5}$FnI with G_{778}–G_{799} showed no binding, indicating that the high-affinity interaction observed is specific. Further experiments with the non-triple-helical N-terminal segment of α_1(I) or a designed

Author contributions: M.C.E., D.A.S., and I.V. designed research; M.C.E., D.A.S., C.J.M., and I.V. performed research; M.C.E., D.A.S., E.D.L., R.W.F., and I.V. analyzed data; and M.C.E., I.D.C., and I.V. wrote the paper.

The authors declare no conflict of interest.

This article is a PNAS Direct Submission.

Freely available online through the PNAS open access option.

Data deposition: The atomic coordinates have been deposited in the Research Collaboratory for Structural Bioinformatics Protein Data Bank (RCSB PDB), www.rcsb.org/pdb (accession no. 3EJH) and the Biological Magnetic Resonance Bank (BMRB), www.bmrb.wisc.edu (accession no. 15986).

[1]To whom correspondence should be addressed. E-mail: ioannis.vakonakis@bioch.ox.ac.uk.

This article contains supporting information online at www.pnas.org/cgi/content/full/0812516106/DCSupplemental.

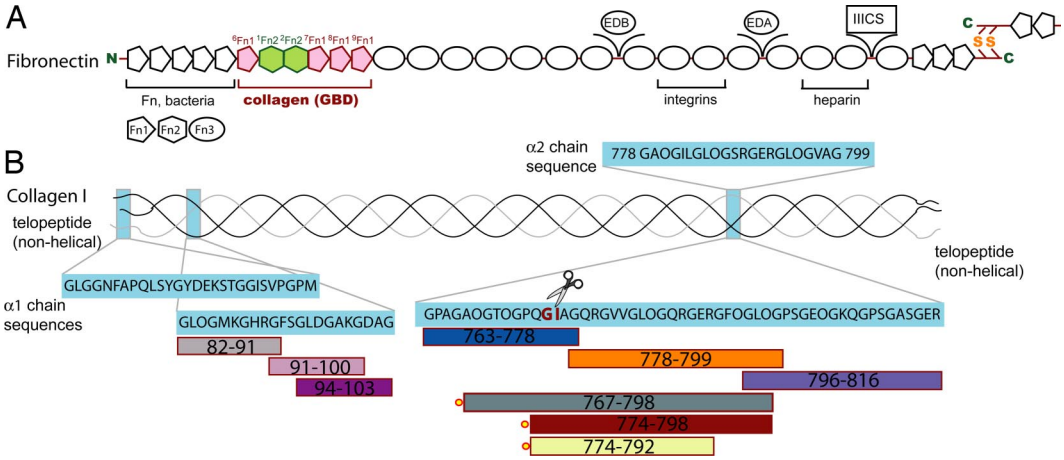

Fig. 1. Schematic representation of fibronectin fragments and collagen-derived peptides. (*A*) Domain structure of human fibronectin, including the alternatively spliced EDB, EDA, and IIICS regions and the dimerization site. The gelatin-binding domain (GBD) is colored according to domain-type (pink, type I; green, type II) and numbered. (*B*) Type I collagen is composed of 2 α_1 (black) and 1 α_2 (gray) chains. Peptides spanning different regions are color coded and fluorescent tags are shown as red circles.

triple-helical GCP(GPP)$_{10}$GCPG peptide also showed no binding to either GBD subfragment.

To test whether intact GBD binds the same collagen site with high affinity, we used a combination of fluorescence anisotropy and NMR. Initial experiments using a α_1(I) peptide N-terminally tagged with 5-carboxyfluorescein, 5-FAM-G$_{778}$–O$_{798}$, showed little binding possibly because of steric interactions with the fluorescent label (Fig. S2). Addition of few N-terminal residues,

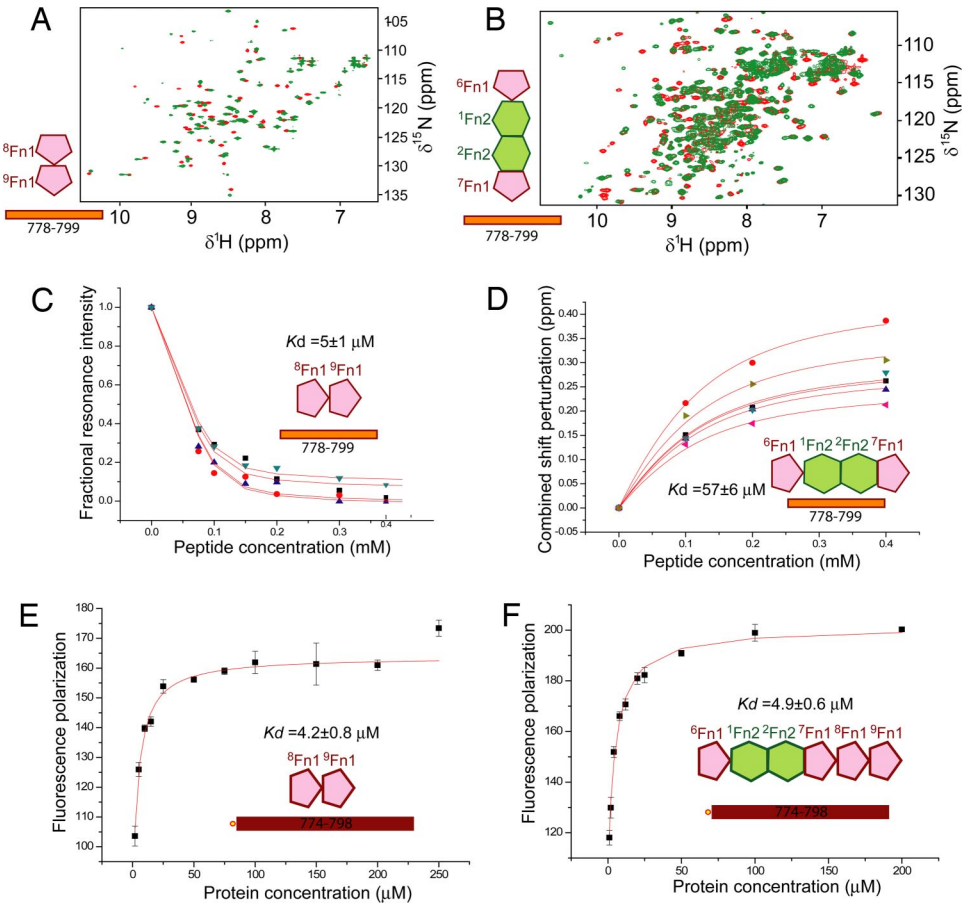

Fig. 2. Interaction of collagen peptides with FN fragments. (*A*) NMR spectra of $^{8-9}$FnI with (red) or without (green) α_1(I) G$_{778}$–G$_{799}$ peptide. (*B*) Analogous spectra of ^{6}FnI$^{1-2}$FnII^{7}FnI. Strong resonance perturbations upon titration are indicative of binding. The ^{6}FnI$^{1-2}$FnII^{7}FnI spectra were collected at 15 °C and 950 MHz where the interaction occurs at the slow NMR time scale. (*C*) Fit of resonance intensities from $^{8-9}$FnI (25 °C) or (*D*) chemical shift perturbations of ^{6}FnI$^{1-2}$FnII^{7}FnI (37 °C) during NMR titrations. (*E*) Fluorescence anisotropy titration of collagen peptide and $^{8-9}$FnI or (*F*) GBD fit to a single binding model.

5-FAM-Q_{774}–O_{798}, resulted in GBD binding with an affinity similar to $^{8-9}$FnI (Fig. 2 *E* and *F* and Table S1); further N-terminal extension did not alter this result (Fig. S2). This lack of increased affinity in the fluorescence titrations indicates that the 2 GBD subfragments do not bind the single-stranded peptide cooperatively; NMR experiments on intact GBD suggest, however, that both subfragments retain their binding potential in the larger context. Specifically, ^{15}N-enriched GBD in the presence of excess G_{778}–G_{799} display resonances characteristic of the bound state of both $^{8-9}$FnI and ^{6}FnI$^{1-2}$FnII^{7}FnI (Fig. S3). Ingham et al. (16) speculated that FN domains bind adjacent segments of collagen in a linear fashion. GBD/collagen models based on our $^{8-9}$FnI complex (see below) and existing structural data on ^{6}FnI$^{1-2}$FnII^{7}FnI (19, 20) suggested such a putative additional site near α_1(I) residue 807. However, peptides spanning that region showed no interaction with ^{6}FnI$^{1-2}$FnII^{7}FnI in NMR titrations (Table S1).

Some evidence (supporting information in ref. 8) suggest that FN interacts equally well with both α_1(I) and α_2(I) chains; therefore, we tested by NMR the equivalent α_2(I) G_{778}–G_{799} sequence for binding the GBD subfragments (Table S1). Compared with α_1(I), this peptide sequence is 71% identical or conservatively substituted over the X/Y positions of the collagen repeat. $^{8-9}$FnI bound this peptide with affinity similar to α_1(I), K_d of 8 ± 2 μM (25 °C) and displayed resonance perturbations in equivalent residues, indicative of similar mode of binding (Fig. S1). In contrast, ^{6}FnI$^{1-2}$FnII^{7}FnI bound the α_2(I) peptide much more weakly that α_1(I), K_d of 3 ± 0.8 mM (37 °C), and showed minimal perturbations. Thus, we conclude that the 2 GBD subfragments bind strongest to collagen at a site adjacent to the MMP-1 cleavage site, albeit with preference for the α_1(I) chain by ^{6}FnI$^{1-2}$FnII^{7}FnI. Although both subfragments retain their affinity to small collagen peptides in the context of the GBD, there is no evidence for cooperative binding to single-stranded chains.

Crystal Structure of $^{8-9}$FnI in Complex with α_1(I) G_{778}–G_{799}. To gain detailed structural insight into the binding of collagen to FN, we crystallized the GBD subfragment that has the highest affinity for our collagen peptide. $^{8-9}$FnI, together with α_1(I) G_{778}–G_{799}, crystallized in space group $P3_121$ with 2 molecules of $^{8-9}$FnI and 2 collagen peptides per asymmetric unit. Datasets, to a maximum resolution of 2.1 Å, were collected at the Diamond Light Source synchrotron facility (Didcot, U.K.); dataset and refinement statistics are shown in Table S2. Both ^{8}FnI and ^{9}FnI exhibit canonical FnI (21, 22) structures (Fig. 3*A*), with a double- and a triple-stranded antiparallel β-sheet (strands A,B and C,D,E, respectively) stabilized by disulfide bonds between strands A/D and D/E. The presence of canonical FnI structures was also confirmed in solution through chemical shift index (23) analysis of the complex assignments. All collagen residues except G_{781} were visible in one of the crystallographic copies whereas, in the other, electron density only allowed V_{782}–G_{796} to be built. In both copies, peptide residues G_{787}–E_{791} align in an antiparallel β-strand fashion along strand E of ^{8}FnI to form an extension of the β-sheet (Fig. 3 *A* and *C*), a mode of interaction commonly seen in protein complexes (24). This type of binding is similar to that of proteins from pathogenic bacteria in complex with FnI modules (Fig. 3*B*) (21, 22), which indicates a functional similarity between the collagen and bacterial protein interactions with FN. It is worth noting that the isolated peptide in solution does not adopt a stable β-strand conformation (Fig. S4).

The peptide conformation is stabilized by specific hydrophobic contacts: The indole ring of ^{8}FnI W_{553} stacks above the peptide main chain over residues R_{789}–G_{790}, and the L_{785} sidechain is sandwiched between those of H_{539} in the loop between strands C and D of ^{8}FnI and F_{569} in strand A of ^{9}FnI (Fig. 4*A*). These 2 hydrophobic interactions account for >27% of the total buried area along this part of the interface. Multiple electrostatic

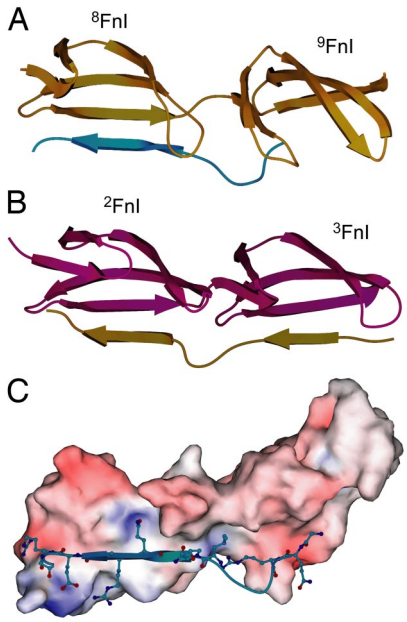

Fig. 3. Overview of the complex structure. (*A*) Schematic representation of the $^{8-9}$FnI module pair in gold and the α_1(I) G_{778}–G_{799} peptide in cyan showing the antiparallel β-strand mode of binding. (*B*) Similar representation of $^{2-3}$FnI (purple) in complex with a peptide (gold) from *Staphylococcus aureus* (21). Collagen and bacterial peptides adopt a similar model of binding to FnI domains. (*C*) Molecular surface area representation of $^{8-9}$FnI colored by electrostatic potential and select collagen peptides residues involved in complex formation.

interactions are made, including 10 hydrogen bonds (O_{786} O′–H_{539} $N^{\varepsilon 2}$, Q_{788} N–C_{555} O′, Q_{788} $N^{\varepsilon 2}$–K_{533} N^{ζ}, Q_{788} O′–C_{555} N, G_{790} N–W_{553} O′, G_{790} O′–W_{553} N, R_{792} N–R_{550} O′, R_{792} $N^{\eta 1}$–Q_{517} O′, R_{792} $N^{\eta 2}$–Q_{549} O′, and R_{792} $N^{\eta 1/2}$–D_{516} $O^{\delta 1}$) and 2 salt-bridges to ^{8}FnI (R_{792}–D_{516} and E_{791}–R_{550}/R_{552}, Fig. 4*B*). Collagen residues N-terminal to the peptide β-strand form 3 hydrogen bonds to strand E of ^{9}FnI (G_{778} N–W_{597} O′, G_{778} O′–W_{597} N, and R_{780} N–I_{594} O′, Fig. 4*C*) increasing the total interface area to ≈725 Å^2, whereas residues C-terminal to R_{792} form a turn, likely through localized hydrophobic collapse of F_{794}, and diverge away from ^{8}FnI. These 6 C-terminal residues participate in 2 further protein–peptide contacts in the crystal lattice (Fig. S5); both of these are smaller than the main interface (430 Å^2 versus 725 Å^2) and rely heavily on the presence of the C-terminal residues for up to 80% of their contact area. Fluorescence anisotropy experiments with a C-terminally truncated peptide (residues Q_{774}–R_{792}) showed only a small effect on affinity (Table S1 and Fig. S2); this suggests that these interfaces are unlikely to form in solution. The pattern of $^{8-9}$FnI chemical shifts induced upon binding is also consistent with an antiparallel β-strand interface forming in solution; resonances at and proximal to ^{8}FnI strand E, for example, the side-chain imino nitrogen of W_{553}, are perturbed upon complex formation.

Multiple Putative $^{8-9}$FnI-Binding Sites in Type I Collagen. We infer from the structural data that the core $^{8-9}$FnI-binding site of collagen comprises the peptide β-strand GLOGQRGER, which includes an integrin-binding motif (25, 26) with moderate affinity for activated cells (27). In addition, this sequence comprises the proposed recognition site (RGER) of MMP-1 that defines the 3/4 region as the site of collagenolysis (28). This sequence is almost identical between the α_1(I) and α_2(I) chains, which would explain their similar affinity to $^{8-9}$FnI shown above. Sequence determinants for binding include a hydrophobic residue in the first triplet and an absence of strand-breaking (proline/4-

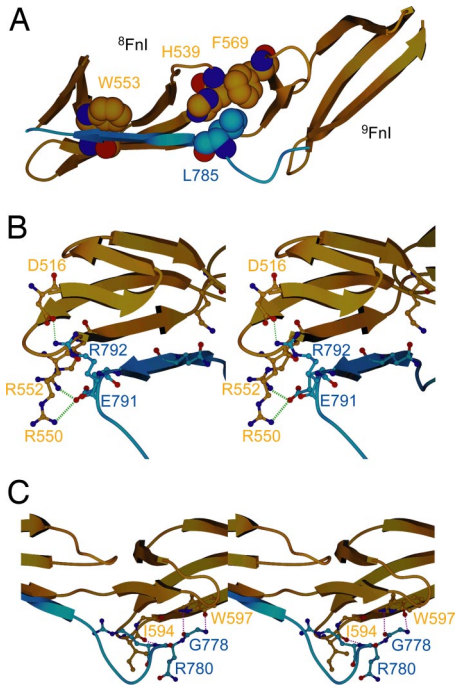

Fig. 4. Details from the molecular interaction of the complex. (*A*) Hydrophobic interactions stabilizing the $^{8-9}$FnI (gold)–peptide (blue) conformation involve W_{553} stacking above the peptide (blue) plane and L_{785} of α_1(I) contacting H_{539} and F_{569}. (*B*) Stereoview of the β-stranded portion of the collagen peptide. Two salt bridges to $^{8-9}$FnI are formed at its C terminus (green dashed lines) as well as important hydrogen bonds among the residues shown. (*C*) Stereoview of the peptide N terminus interacting with ^{9}FnI, primarily through hydrogen bonds (red dashed lines).

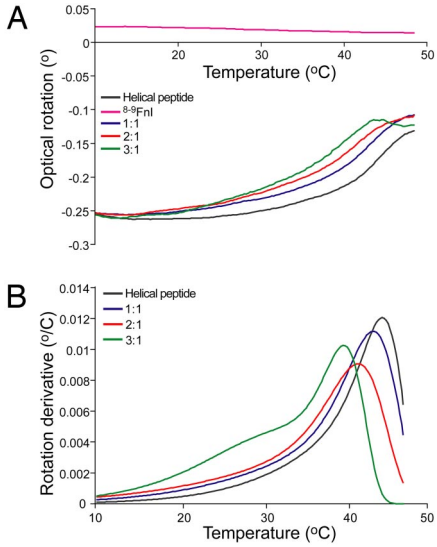

Fig. 5. $^{8-9}$FnI destabilizes the triple-helical structure. Denaturation of 0.05 mM helix alone or in the presence of $^{8-9}$FnI, denoted as $^{8-9}$FnI/helix ratios, was monitored by optical rotation (*A*). A control sample of 0.05 mM $^{8-9}$FnI alone is shown in purple. (*B*) Fits to derivative of optical rotation with respect to temperature derived by using D/z kinetic approximations (30). The main maxima provide the helical melting temperature (T_m).

hydroxyproline) residues in the next 2 repeats. This basic 9-mer pattern is found 11 times in collagen α_1(I) and 17 times in α_2(I) (Table S3), consistent with earlier studies that demonstrated multiple FN-binding sites in collagen chain fragments (9). However, variations in the amino acid sequence can influence the observed affinity; in particular positions 2 (L) and 9 (R) are sensitive even to conservative substitutions. Replacement of these residues by F and K leads to substantial decrease in the observed affinity (Table S1 and Fig. S6), possibly because of steric clashes and alterations in hydrogen bonding patterns, respectively. Interestingly, examination of the 9-mer patterns of α_1(I) and α_2(I) reveals only 2 sites per chain that fulfill all these criteria for enhanced binding (Table S3), and in both cases, the α_1(I) and α_2(I) sites lie next to each other in the collagen triple helix (29). This likely creates 2 hot spots for potential FN binding in the collagen sequence and may affect tissue organization and architecture.

We performed NMR titrations with peptides corresponding to 3 of the predicted binding sites that cluster between α_1(I) residues 82 and 102 (Table S3). Only 1 of these, GLOGMKGHR, showed an affinity for $^{8-9}$FnI that is comparable with that of GLOGQRGER (Table S1 and Fig. S6) under the conditions used (37 °C). The remaining 2 peptides, GFSGLDGAK and GLDGAKGDA, bound very weakly. Mixtures of all 3 peptides to $^{8-9}$FnI under similar stoichiometric ratios at 25 °C are shown in Fig. S7. The extent of chemical shift perturbations induced varies; GFSGLDGAK and GLDGAKGDA caused the smallest perturbations, indicative of their reduced affinities. This result is in agreement with our earlier efforts to identify critical residues in the 9-mer pattern, and the variable affinities of the putative 9-mer patterns identified in collagen likely influence the apparent binding and kinetics observed between denatured collagen and FN (18).

$^{8-9}$FnI Destabilizes the Collagen Triple Helix in Vitro. The extended conformation adopted by the collagen peptide bound to $^{8-9}$FnI suggests that interaction with FN may alter the local structure of collagen (29), either by stabilizing the small fraction of unwound collagen or by inducing a non-triple-helical conformation. In either case the local equilibrium would be shifted toward the unwound collagen state. To test this hypothesis, we monitored the thermal stability of a FN-binding triple-helical peptide from the homotrimeric type II collagen, using optical polarimetry (Fig. 5). The peptide sequence, GPC(GPP)$_5$GLAGQRGIVGLOGQRGERGFOGLOGPS(GPP)$_5$GPC, includes the MMP-1 cleavage site and differs from the equivalent collagen I sequence (Table S1) by 2 conservatively substituted residues, L instead of I in the first collagen triple repeat and I instead of V in the third. Samples of 0.05 mM triple helix alone or in the presence of stoichiometric ratios of $^{8-9}$FnI were thermally denatured up to 50 °C; the change in melting temperature (T_m) was estimated by fitting the data by using kinetic approximations (30). The polarimetric properties of $^{8-9}$FnI did not change over the range of temperatures used, and previous studies have reported a T_m of ≈65 °C for this module pair (31). As seen in Fig. 5, $^{8-9}$FnI destabilized the triple-helical conformation in a concentration-dependent manner up to ≈5 °C under the conditions used; experiments at higher (0.1 mM) triple-helix concentrations and similar $^{8-9}$FnI stoichiometric ratios showed increased destabilization of 10 °C. Because the MMP-1 site is relatively labile at near-physiological temperatures, this observed FN-induced destabilization is likely to increase substantially the fraction of unfolded collagen.

Discussion

We present structural evidence for a direct FN–collagen interaction. The identified site, G_{778}–G_{799}, lies adjacent to the MMP-1 cleavage site, in agreement with earlier data from cell culture assays (6, 14, 15). Interestingly, the peptide adopts a conformation in the $^{8-9}$FnI complex similar to that of bacterial peptides in

complex with FN (21, 22). The GBD is known to associate with segments of these bacterial proteins (32, 33) raising the possibility of competition with collagen for FN binding. Such binding could have significant functional implications for tissue changes induced during bacterial colonization. On the other hand, it has been shown that *Streptococcus pyogenes* colonize collagen type I fibers in vitro only after pretreatment with FN (34). It is thus tempting to speculate that bacteria might hijack the FN–collagen interaction to evade the host's immune system through deposition of matrix components on the bacterial surface.

The GBD subfragments bind strongly to α_1(I) G_{778}–G_{799} but only $^{8-9}$FnI associates with the equivalent segment of the α_2(I) chain. We believe this result may be interesting in light of preferential α_2(I) cleavage by MMP-1 (28, 35, 36) and possible $^{8-9}$FnI implications on collagenolysis (see below). Single-stranded α_1(I) peptide binding to GBD is not cooperative. However, we showed that both GBD subfragments can simultaneously bind collagen peptides, and this may lead to GBD associating strongly with the heterotrimeric triple helix or with individual chains from multiple collagen strands. This scenario is more likely in situ, because the local concentration of these strands will be high and could involve different microfibrils. This avidity effect could also explain the tight affinity of GBD for gelatin (18), where multiple independent strands are accessible.

Upon binding, $^{8-9}$FnI destabilizes the local collagen conformation by linearizing 1 chain and, possibly, increasing accessibility of the other 2 chains. Previous studies have noted that the segment surrounding the collagenase/MMP-1 (13) cleavage site may be partly unfolded at physiological temperatures (35, 37, 38), and MMP-1 is believed to require local unwinding of the collagen triple helix for cleavage (35). Collagenolysis does not, however, require any energy input (35); instead a thermodynamic mechanism involving specific MMP-1 binding to this site has been proposed (39). The MMP-1 hemopexin domain is likely involved in this mechanism (35), and its proposed recognition site, RGER (28), overlaps with the $^{8-9}$FnI-binding site identified here. Thus, we believe there may be a functional overlap between the MMP-1 hemopexin domain and $^{8-9}$FnI, because both alter the local conformation of this collagen site.

Accessibility of sites in the collagen fibril is restricted compared with isolated triple helices because of molecular packing; however, cleavage of the C-telopeptide exposes collagenase sites within the fibril and allows efficient processing by MMP-1 (28). This process should also allow FN access to the collagenase site. Models of fibril proteolysis suggest that MMP-1 engages collagen near the core $^{8-9}$FnI-binding sequence identified here before preferential α_2(I) cleavage (28, 35, 36) and that molecular interactions can regulate enzymatic activity in vivo (28). The in situ effect of FN–collagen interactions adjacent to the MMP-1 site is hard to predict, because FN may enhance cleavage through increase site accessibility or, in contrast, may sterically inhibit further proteolysis and facilitate cellular attachment to partially digested fibrils (40). It is likely that the ultimate result will vary with tissue type and developmental stage because it would depend on both the relative abundance of collagen, FN, and MMPs and the presence of other interacting molecules such as integrins and discoidin domain receptors (2, 41). In light of the importance of MMP activity during invasive migration in tumor progression (42), the potential regulatory role of FN inferred here opens avenues of understanding that may lead to therapeutic advance.

Materials and Methods

Material Production and Purification. FN fragments correspond to residues 305–608 (GBD), 305–515 (^{6}FnI$^{1-2}$FnII^{7}FnI), and 516–608 ($^{8-9}$FnI). $^{8-9}$FnI and GBD are N528Q/R534K substituted (17). Recombinant proteins were produced and purified as described (17, 43). Briefly, constructs encoding the desired FN fragments were integrated in the *AOX1* genetic locus and expressed proteins were secreted. These were concentrated from the media by cation exchange chromatography and further purified by reverse phase and size exclusion chromatography (^{6}FnI$^{1-2}$FnII^{7}FnI, $^{8-9}$FnI), or gelatin affinity chromatography (GBD). Synthetic single-stranded peptides were purchased from GL Biochem; their sequences are provided in Table S1 and, unless fluorescently tagged, included a C-terminal tyrosine residue for UV determination of peptide concentration. Fluorescent peptides had 5-carboxyfluorescein attached to the N-terminal amine group. The triple-helical peptide from the α_1(II) chain was synthesized as described (44), thermally denatured and allowed to refold for 48 h at 8 °C.

NMR Spectroscopy. NMR spectrometers used Oxford Instruments superconducting magnets with 11.7- or 22.3-T magnetic field strengths and home-built or Bruker Avance II consoles. Spectra were recorded in a 20 mM Na_2HPO_4 (pH 7.2) (^{6}FnI$^{1-2}$FnII^{7}FnI) or PBS, 20 mM Na_2HPO_4 (pH 7.2), 150 mM NaCl ($^{8-9}$FnI, GBD) sample buffer. Magnetic fields and temperatures used were in all cases optimized to avoid resonance broadening because of intermediate exchange, but generally correspond to 25 °C ($^{8-9}$FnI) or 37 °C (^{6}FnI$^{1-2}$FnII^{7}FnI, GBD) unless otherwise noted. Sequential chemical shift assignments of $^{8-9}$FnI in complex with α_1(I) G_{776}–G_{799} were performed by using standard triple-resonance experiments. Analysis of spectral perturbations upon protein interactions and determination of equilibrium parameters were performed as described (43).

Fluorescence Anisotropy Experiments. Fluorescence anisotropy measurements were performed at 25 °C in a 20 mM Tris-Cl (pH 7.4), 150 mM NaCl buffer (TBS) by using a SpectraMax M5 fluorimeter (Molecular Devices). Samples of 75 nM labeled peptide and increasing concentrations of protein in 96-well plates were excited at 485 nm with a 515-nm cutoff, and fluorescence was observed at 538 nm. Differences in fluorescence anisotropy were fit by using a single binding model (43). Error bars are derived from triplicate experiments.

X-Ray Crystallography. Crystals of the $^{8-9}$FnI–α_1(I) peptide complex formed by using the vapor-diffusion method from sitting drops dispensed by a mosquito Crystal robot (TPP LabTech). The drops consisted of 100 nL of an equimolar mixture of protein (20 mg/mL) and α_1(I) peptide in 10 mM Hepes, 50 mM NaCl (pH 7.0), and 100 nL of reservoir solution of 2.5 M NaCl, 0.1 M BisTris (pH 6.5). Crystals were cryoprotected by transfer to a reservoir solution supplemented by 25% vol/vol glycerol and flash frozen. Initial in-house diffraction data were recorded by using a Bruker SMART 6000 CCD detector installed on a 2.7-kW MicroStar X-ray generator, and data were integrated and scaled by using Proteum2. Synchrotron data at 2.1-Å resolution were integrated with MOSFLM and scaled with Scala. The structure was solved by molecular replacement by using Phaser (45) with a superimposed ensemble of FnI crystal structures (PDB ID codes 2CG6 and 2CG7) as search model. Refinement was performed in PHENIX (46) by using noncrystallographic symmetry restraints between parts of chains A and B (protein), and E and F (peptide) of the complex and TLS refinement with 1 group per FnI domain or peptide polypeptide chain. Manual model building was performed in Coot (47).

Optical Polarimetry. Triple-helix stability in 150 mM NaCl, 20 mM Tris-Cl (pH 7.4) (TBS) buffer was assessed by using an Autopol III polarimeter with 10-cm path length. Samples of triple-helical peptide or peptide–protein mixtures were degassed with nitrogen before use. Sample temperature was varied by 1 °C/min from 8 to 50 °C. The signal from a control sample of 0.05 mM $^{8-9}$FnI alone (Fig. 5) was appropriately subtracted from those of sample mixtures to derive the optical rotation of the triple helix. Data noise was reduced by averaging over a 2.5 °C sliding window. The first derivative of the data was mathematically fitted to 2 events by using D/z kinetic approximations (30). Circular dichroism spectra were collected at 25 °C in a 150 mM NaCl, 20 mM Na_2HPO_4 (pH 7.2) buffer by using a Jasco J-720 Spectropolarimeter with 0.1-cm path length.

Note. Amino acid numbering for FN corresponds to UniProt entry P02751. α_1(I) and α_2(I) numbering is taken to start from the estimated start of the helical region. ''O'' in peptide sequences denotes 4-hydroxyproline. Interactions between $^{8-9}$FnI and the collagen peptide were analyzed with the PISA service from the European Bioinformatics Institute (48). Structural data have been deposited in the Research Collaboratory for Structural Bioinformatics (RCSB) under accession no. 3EJH for the $^{8-9}$FnI–α_1(I) peptide complex. NMR chemical shift assignments of the complex have been deposited in the BioMagResBank under accession no. 15986.

ACKNOWLEDGMENTS: Funding was provided by the Wellcome Trust and Royal Society. We thank the Medical Research Council for support toward peptide synthesis and Bruker AXS for the CCD detector loan. M.C.E. thanks the Swiss National Foundation. D.A.S. thanks the British Heart Foundation. I.V. acknowledges support from the Marie Curie Fellowships and Trinity College, Oxford.

1. Leitinger B, Hohenester E (2007) Mammalian collagen receptors. *Matrix Biol* 26:146–155.
2. Kadler KE, Hill A, Canty-Laird EG (2008) Collagen fibrillogenesis: Fibronectin, integrins, and minor collagens as organizers and nucleators. *Curr Opin Cell Biol* 20:495–501.
3. Vakonakis I, Campbell ID (2007) Extracellular matrix: From atomic resolution to ultrastructure. *Curr Opin Cell Biol* 19:578–583.
4. Pankov R, Yamada KM (2002) Fibronectin at a glance. *J Cell Sci* 115:3861–3863.
5. Mao Y, Schwarzbauer JE (2005) Fibronectin fibrillogenesis, a cell-mediated matrix assembly process. *Matrix Biol* 24:389–399.
6. Dessau W, Adelmann BC, Timpl R (1978) Identification of the sites in collagen alpha-chains that bind serum anti-gelatin factor (cold-insoluble globulin). *Biochem J* 169:55–59.
7. Engvall E, Ruoslahti E (1977) Binding of soluble form of fibroblast surface protein, fibronectin, to collagen. *Int J Cancer* 20:1–5.
8. Ingham KC, Brew SA, Isaacs BS (1988) Interaction of fibronectin and its gelatin-binding domains with fluorescent-labeled chains of type I collagen. *J Biol Chem* 263:4624–4628.
9. Ingham KC, Brew SA, Migliorini M (2002) Type I collagen contains at least 14 cryptic fibronectin binding sites of similar affinity. *Arch Biochem Biophys* 407:217–223.
10. Balian G, Click EM, Bornstein P (1980) Location of a collagen-binding domain in fibronectin. *J Biol Chem* 255:3234–3236.
11. Hynes R (1985) Molecular biology of fibronectin. *Annu Rev Cell Biol* 1:67–90.
12. McDonald JA, Kelley DG, Broekelmann TJ (1982) Role of fibronectin in collagen deposition: Fab′ to the gelatin-binding domain of fibronectin inhibits both fibronectin and collagen organization in fibroblast extracellular matrix. *J Cell Biol* 92:485–492.
13. Iyer S, Visse R, Nagase H, Acharya KR (2006) Crystal structure of an active form of human MMP-1. *J Mol Biol* 362:78–88.
14. Kleinman HK, McGoodwin EB (1976) Localization of the cell attachment region in types I and II collagens. *Biochem Biophys Res Commun* 72:426–432.
15. Kleinman HK, et al. (1978) Localization of the binding site for cell attachment in the alpha1(I) chain of collagen. *J Biol Chem* 253:5642–5646.
16. Ingham KC, Brew SA, Migliorini MM (1989) Further localization of the gelatin-binding determinants within fibronectin. Active fragments devoid of type II homologous repeat modules. *J Biol Chem* 264:16977–16980.
17. Millard CJ, Campbell ID, Pickford AR (2005) Gelatin binding to the 8F19F1 module pair of human fibronectin requires site-specific *N*-glycosylation. *FEBS Lett* 579:4529–4534.
18. Katagiri Y, Brew SA, Ingham KC (2003) All six modules of the gelatin-binding domain of fibronectin are required for full affinity. *J Biol Chem* 278:11897–11902.
19. Baron M, Norman D, Willis A, Campbell ID (1990) Structure of the fibronectin type 1 module. *Nature* 345:642–646.
20. Pickford AR, Smith SP, Staunton D, Boyd J, Campbell ID (2001) The hairpin structure of the (6)F1(1)F2(2)F2 fragment from human fibronectin enhances gelatin binding. *EMBO J* 20:1519–1529.
21. Bingham RJ, et al. (2008) Crystal structures of fibronectin-binding sites from *Staphylococcus aureus* FnBPA in complex with fibronectin domains. *Proc Natl Acad Sci USA* 105:12254–12258.
22. Schwarz-Linek U, et al. (2003) Pathogenic bacteria attach to human fibronectin through a tandem beta-zipper. *Nature* 423:177–181.
23. Wishart DS, Sykes BD, Richards FM (1992) The chemical shift index: A fast and simple method for the assignment of protein secondary structure through NMR spectroscopy. *Biochemistry* 31:1647–1651.
24. Remaut H, Waksman G (2006) Protein–protein interaction through beta-strand addition. *Trends Biochem Sci* 31:436–444.
25. Emsley J, Knight CG, Farndale RW, Barnes MJ, Liddington RC (2000) Structural basis of collagen recognition by integrin alpha2beta1. *Cell* 101:47–56.
26. Xu Y, et al. (2000) Multiple binding sites in collagen type I for the integrins alpha1beta1 and alpha2beta1. *J Biol Chem* 275:38981–38989.
27. Siljander PR, et al. (2004) Integrin activation state determines selectivity for novel recognition sites in fibrillar collagens. *J Biol Chem* 279:47763–47772.
28. Perumal S, Antipova O, Orgel JP (2008) Collagen fibril architecture, domain organization, and triple-helical conformation govern its proteolysis. *Proc Natl Acad Sci USA* 105:2824–2829.
29. Orgel JP, Irving TC, Miller A, Wess TJ (2006) Microfibrillar structure of type I collagen in situ. *Proc Natl Acad Sci USA* 103:9001–9005.
30. Miles CA, Bailey AJ (2004) Studies of the collagen-like peptide (Pro-Pro-Gly)(10) confirm that the shape and position of the type I collagen denaturation endotherm is governed by the rate of helix unfolding. *J Mol Biol* 337:917–931.
31. Litvinovich SV, Strickland DK, Medved LV, Ingham KC (1991) Domain structure and interactions of the type I and type II modules in the gelatin-binding region of fibronectin. All six modules are independently folded. *J Mol Biol* 217:563–575.
32. Ozeri V, et al. (1996) A two-domain mechanism for group A streptococcal adherence through protein F to the extracellular matrix. *EMBO J* 15:989–998.
33. Talay SR, et al. (2000) Co-operative binding of human fibronectin to Sfbl protein triggers streptococcal invasion into respiratory epithelial cells. *Cell Microbiol* 2:521–535.
34. Dinkla K, et al. (2003) *Streptococcus pyogenes* recruits collagen via surface-bound fibronectin: A novel colonization and immune evasion mechanism. *Mol Microbiol* 47:861–869.
35. Chung L, et al. (2004) Collagenase unwinds triple-helical collagen prior to peptide bond hydrolysis. *EMBO J* 23:3020–3030.
36. Muller JC, Ottl J, Moroder L (2000) Heterotrimeric collagen peptides as fluorogenic collagenase substrates: Synthesis, conformational properties, and enzymatic digestion. *Biochemistry* 39:5111–5116.
37. Fiori S, Sacca B, Moroder L (2002) Structural properties of a collagenous heterotrimer that mimics the collagenase cleavage site of collagen type I. *J Mol Biol* 319:1235–1242.
38. Stultz CM (2002) Localized unfolding of collagen explains collagenase cleavage near imino-poor sites. *J Mol Biol* 319:997–1003.
39. Nerenberg PS, Salsas-Escat R, Stultz CM (2008) Do collagenases unwind triple-helical collagen before peptide bond hydrolysis? Reinterpreting experimental observations with mathematical models. *Proteins* 70:1154–1161.
40. Di Lullo GA, Sweeney SM, Korkko J, Ala-Kokko L, San Antonio JD (2002) Mapping the ligand-binding sites and disease-associated mutations on the most abundant protein in the human, type I collagen. *J Biol Chem* 277:4223–4231.
41. Konitsiotis AD, et al. (2008) Characterization of high affinity binding motifs for the discoidin domain receptor DDR2 in collagen. *J Biol Chem* 283:6861–6868.
42. Friedl P, Wolf K (2008) Tube travel: The role of proteases in individual and collective cancer cell invasion. *Cancer Res* 68:7247–7249.
43. Vakonakis I, Langenhan T, Promel S, Russ A, Campbell ID (2008) Solution structure and sugar-binding mechanism of mouse latrophilin-1 RBL: A 7TM receptor-attached lectin-like domain. *Structure (London)* 16:944–953.
44. Slatter DA, Foley LA, Peachey AR, Nietlispach D, Farndale RW (2006) Rapid synthesis of a register-specific heterotrimeric type I collagen helix encompassing the integrin alpha2beta1 binding site. *J Mol Biol* 359:289–298.
45. Zwart PH, et al. (2008) Automated structure solution with the PHENIX suite. *Methods Mol Biol* 426:419–435.
46. Adams PD, et al. (2002) PHENIX: Building new software for automated crystallographic structure determination. *Acta Crystallogr D* 58:1948–1954.
47. Emsley P, Cowtan K (2004) Coot: Model-building tools for molecular graphics. *Acta Crystallogr D* 60:2126–2132.
48. Krissinel E, Henrick K (2007) Inference of macromolecular assemblies from crystalline state. *J Mol Biol* 372:774–797.